Snapshots of Dynamical Evolution of Attractors from Chua's Oscillator

Philippe Kévorkian

Abstract—**Chua's oscillator is the *simplest* circuit with the *most complex* chaotic dynamics in the universe of all 21-parameter family $\mathcal{C}$ of continuous odd-symmetric piecewise-linear vector-fields. Consequently, an in-depth understanding of this circuit suffices to explain the nonlinear dynamics of all chaotic circuits and systems belonging to $\mathcal{C}$. Our goal in this *tutorial* is to present a sequence of snapshots that shows the detailed dynamical evolution that led to the birth of distinct *strange attractors* corresponding to several standard routes to chaos.**

I. Introduction

BY ADDING a *linear* resistor R_0 in series with the inductor in Chua's circuit [1], we obtain an unfolded circuit [2], [3] called Chua's oscillator [4]–[6]. This circuit is *canonical* in the sense that it contains the *smallest* number (seven) of circuit parameters *necessary* to exhibit *all possible* nonlinear dynamics and chaotic behaviors that can be obtained from a 21-parameter family $\mathcal{C}$ [2] of continuous odd-symmetric piecewise-linear vectorfields. The canonical property of this circuit is proved in [2], [3]. More than 30 distinct strange attractors exhibited by this circuit have been found to date. Because of the canonical nature of Chua's oscillator, it is the circuit of choice for an in-depth study. In particular, all standard routes to chaos are exhibited by this circuit in different regions of the parameter space. Our goal in this tutorial is to select each of these standard routes to chaos and observe its dynamical evolution by showing a sequence of snapshots of the associated trajectory. Because of the piecewise-linear nature of Chua's oscillator, its many qualitatively distinct dynamical evolutions can be understood by following the evolutions of the corresponding eigenvectors and eigenspaces in the affine region D_1, D_0, and D_{-1}, respectively. Consequently, the location and position of the eigenvectors and eigenspaces are given along with the attractors in the snapshots. Because of space limitation, no explanations, except for the figure captions, are given for these snapshots, which in most cases are self-explanatory.

The Chua's oscillator circuit shown in Fig. 1(a) is described by the following system of third-order ordinary differential equations

$$\begin{cases} C_1\dot{v}_1 = \frac{1}{R}(v_2 - v_1) - \hat{f}(v_1) \\ C_2\dot{v}_2 = \frac{1}{R}(v_1 - v_2) + i_3 \\ L\dot{i}_3 = -v_2 - R_0 i_3 \end{cases} \tag{1}$$

Manuscript received May 2, 1993; revised manuscript received June 22, 1993. This paper was recommended by Guest Editor L. O. Chua.

P. Kevorkian is with l'Ecole Nationale Supérieure de l'Aéronautique et de l'Espace, Toulouse, France.

IEEE Log Number 9211613.

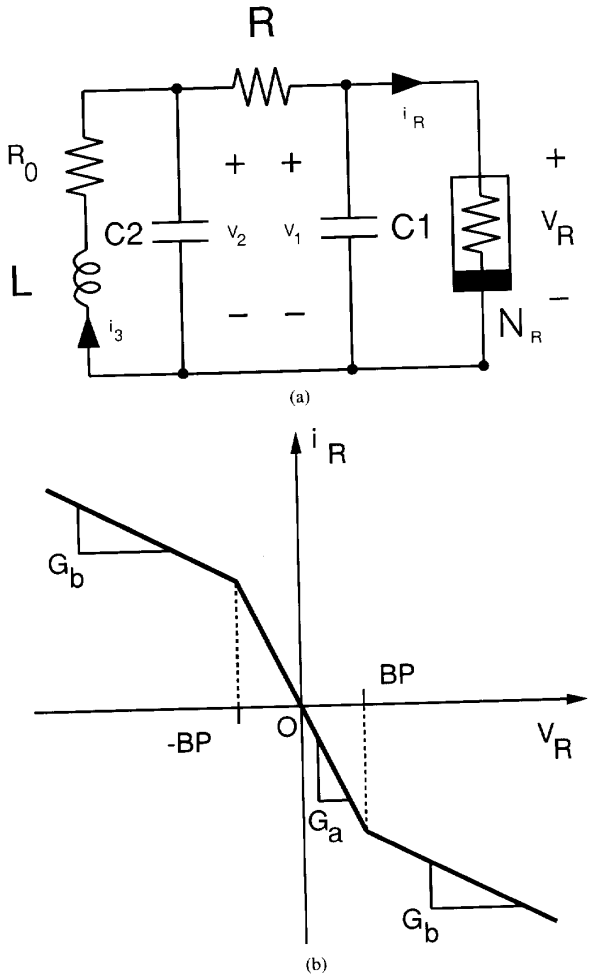

Fig. 1. (a) Chua's oscillator circuit. (b) Example of a piecewise-linear characteristic for Chua's diode.

where C_1, C_2, L, R, and R_0 are real numbers, and

$$\hat{f}(v_R) = G_b v_R + \tfrac{1}{2}(G_a - G_b)[|v_R + B_p| - |v_R - B_p|] \tag{2}$$

denotes the three-segment odd-symmetric *voltage-current* characteristic of the nonlinear resistor (known as Chua's diode [7]) with slopes G_a, G_b and breakpoints located at $v_R = -B_p$ and $v_R = B_p$, respectively. By different choices of G_a and G_b, all combinations of odd-symmetric three-segment characteristics are possible [7], one of which is shown in Fig. 1(b). By an appropriate change of variables, we can transform

TABLE I
PARAMETERS FOR THE SNAPSHOTS

Fig.	α	β	γ	a	b	k
2 through 4	9.8	16	0	−1.1428571	−0.71428571	1
5	8.8	16	0.5	−1.1428571	−0.71428571	1
6(a)	8.8	16	0	−1.1428571	−0.71428571	1
6(b)	9.05	16	0	−1.1428571	−0.71428571	1
7(a)	9.12	16	0	−1.1428571	−0.71428571	1
7(b)	9.162	16	0	−1.1428571	−0.71428571	1
8(a)	9.3	16	0	−1.1428571	−0.71428571	1
8(b)	9.8	16	0	−1.1428571	−0.71428571	1
9(a)	−75.018755	59.988002	−5.9988002	−0.98	−2.4	1
9(b)	−75.018755	44.802867	−4.4802867	−0.98	−2.4	1
10(a)	−75.018755	43.994721	−4.3994721	−0.98	−2.4	1
10(b)	−75.018755	34.722222	−3.4722222	−0.98	−2.4	1
11(a)	−75.018755	31.746032	−3.1746032	−0.98	−2.4	1
11(b)	−75.018755	31.25	−3.125	−0.98	−2.4	1
12(a)	100	1499.2504	−0.97601199	−0.856	−1.1	−1
12(b)	166.66667	1499.2504	−0.97601199	−0.856	−1.1	−1
13(a)	196.07843	1499.2504	−0.97601199	−0.856	−1.1	−1
13(b)	200	1499.2504	−0.97601199	−0.856	−1.1	−1
14(a)	285.71429	1499.2504	−0.97601199	−0.856	−1.1	−1
14(b)	340.13605	1499.2504	−0.97601199	−0.856	−1.1	−1
15	11.5996022	15	0	−1.1428571	−0.71428571	1
16	10.3358877466415610077619	15	0	−1.1428571	−0.71428571	1
17	8.6	13.925	0	−1.1428571	0.71428571	1
18	8.6	13.924	0	−1.1428571	0.71428571	1
19	8.6	13.923	0	−1.1428571	0.71428571	1
20	8.6	13.833	0	−1.1428571	0.71428571	1

(1) and (2) into the following *dimensionless* Chua's equations:

$$\begin{cases} \dot{x} = k\alpha(y - x - f(x)) \\ \dot{y} = k(x - y + z) \\ \dot{z} = k(-\beta y - \gamma z) \end{cases} \tag{3}$$

$$f(x) = bx + \tfrac{1}{2}(a - b)[|x + 1| - |x - 1|] \tag{4}$$

where

$$x = \frac{v_1}{B_p},\ y = \frac{v_2}{B_p},\ z = i_3\left(\frac{R}{B_p}\right)$$
$$\alpha = \frac{C_2}{C_1},\ \beta = \frac{R^2 C_2}{L},\ \gamma = \frac{RR_0C_2}{L}$$
$$a = RG_a, b = RG_b, k = sgn(RC_2) \text{ and } \tau = \frac{t}{|RC_2|} \tag{5}$$

II. EXPLICIT EQUATIONS FOR PLOTTING EIGENVECTORS AND EIGENPLANES

2.1. Equilibrium Points

The equilibrium points of the Chua's oscillator dimensionless equations are determined by solving the following system of equations:

$$\begin{cases} y - x - f(x) = 0 \\ x - y + z = 0 \\ -\beta y - \gamma z = 0 \end{cases} \tag{6}$$

There are three equilibrium points; namely, $\boldsymbol{P}^+ \in D_1$ $(x \geq 1)$, $\boldsymbol{O} \in D_0$ $(-1 \leq x \leq 1)$, and $\boldsymbol{P}^- \in D_{-1}$ $(x \leq -1)$ where

$$\boldsymbol{P}^+ = \begin{bmatrix} x_{eq} \\ \frac{\gamma}{\beta+\gamma}x_{eq} \\ -\frac{\beta}{\beta+\gamma}x_{eq} \end{bmatrix},\ \boldsymbol{O} = \begin{bmatrix} 0 \\ 0 \\ f0 \end{bmatrix},$$
$$\boldsymbol{P}^- = \begin{bmatrix} -x_{eq} \\ -\frac{\gamma}{\beta+\gamma}x_{eq} \\ \frac{\beta}{\beta+\gamma}x_{eq} \end{bmatrix} \tag{7}$$

and

$$x_{eq} = \frac{b - a}{b + \frac{\beta}{\beta+\gamma}} \tag{8}$$

2.2. Eigenvalues

In the *inner* region D_0, the state equation (3) reduces to

$$\dot{\boldsymbol{X}} = \boldsymbol{M_0 X} \tag{9}$$

The Jacobian matrix associated with (9) is the constant matrix

$$\boldsymbol{M_0} = k\begin{pmatrix} -\alpha(1 - a) & \alpha & 0 \\ 1 & -1 & 1 \\ 0 & -\beta & -\gamma \end{pmatrix} \tag{10}$$

whose characteristic polynomial is given by:

$$\lambda^3 + k[1 + \gamma + \alpha(1 + a)]\lambda^2 + [\gamma + \beta + \alpha(1 + \alpha)(1 + \gamma) - \alpha]\lambda + k\alpha[(1 + a)(\gamma + \beta) - \gamma] = 0 \tag{11}$$

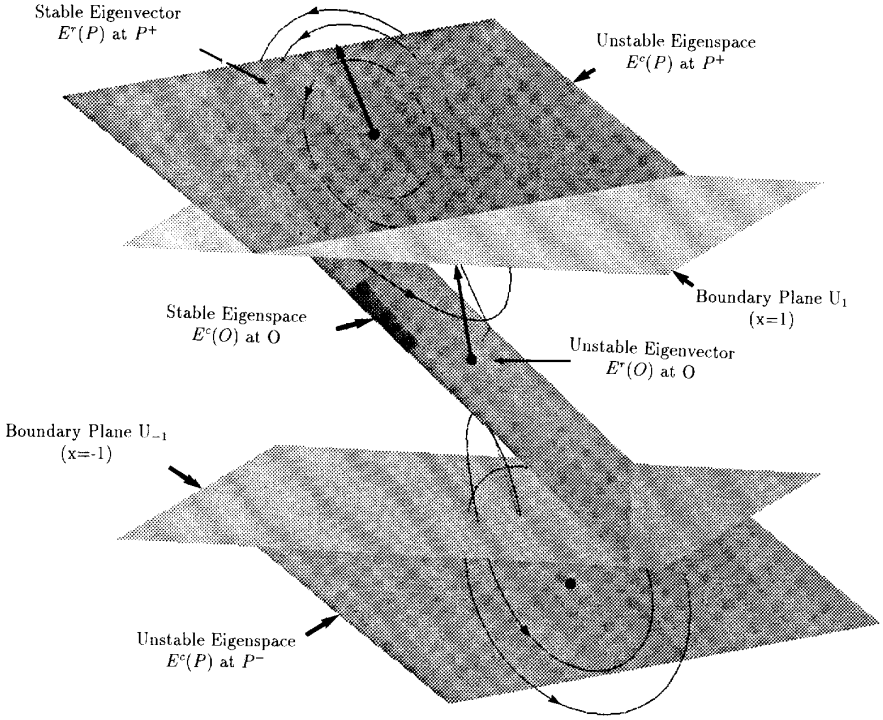

Fig. 2. (a) Trajectory after 300 points.

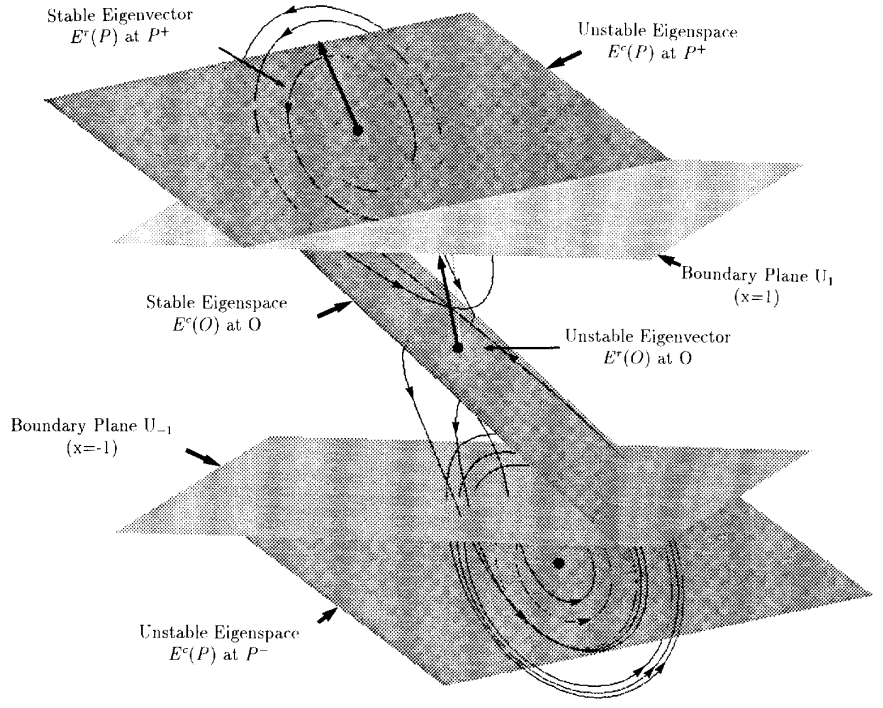

Fig. 2. (b) Trajectory after 600 points.

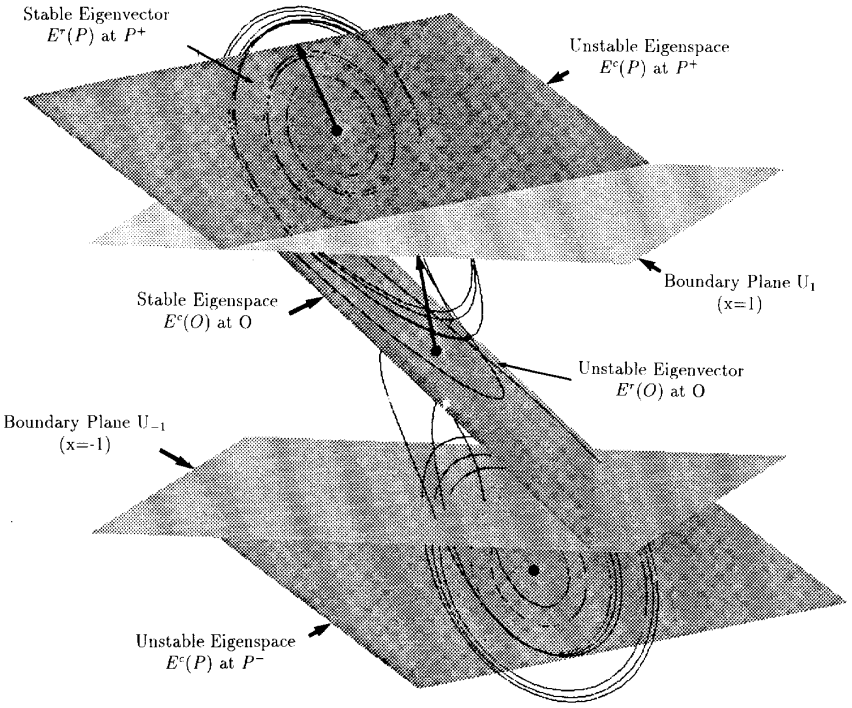

Fig. 3. (a) Trajectory after 900 points.

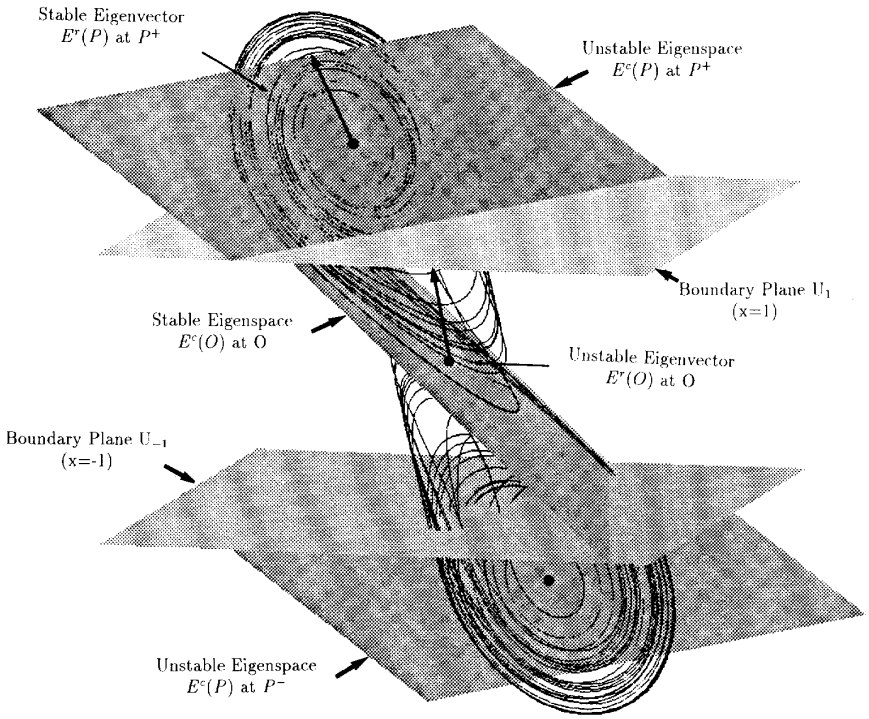

Fig. 3. (b) Trajectory after 2500 points.

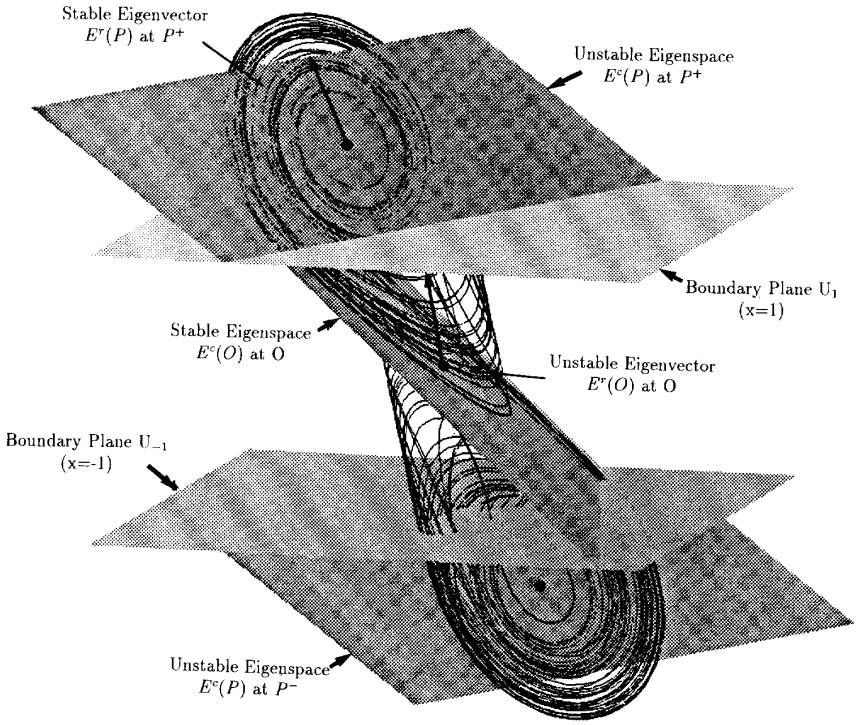

Fig. 4. (a) Trajectory after 5000 points.

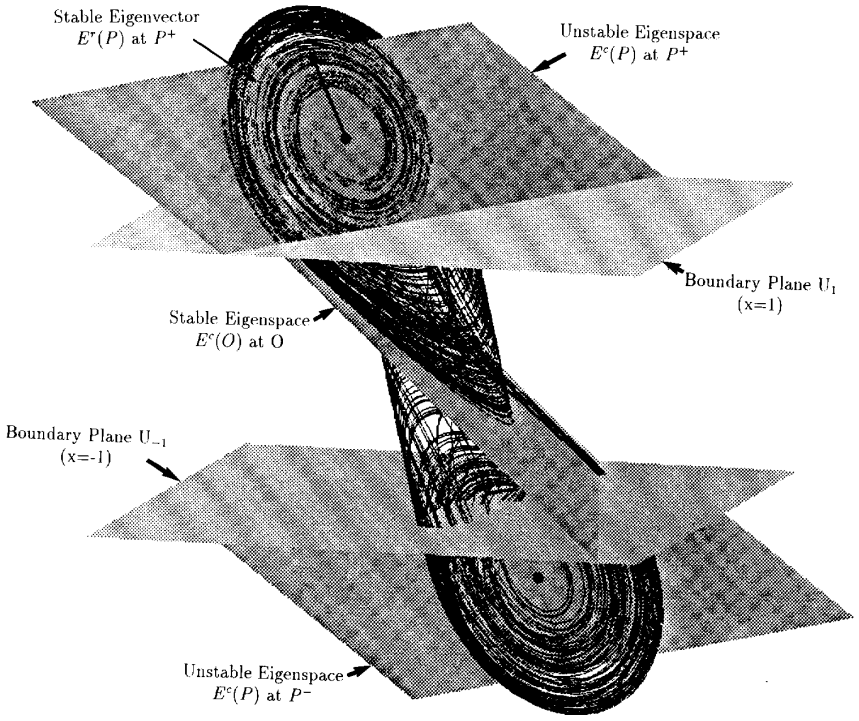

Fig. 4. (b) Trajectory after 15 000 points.

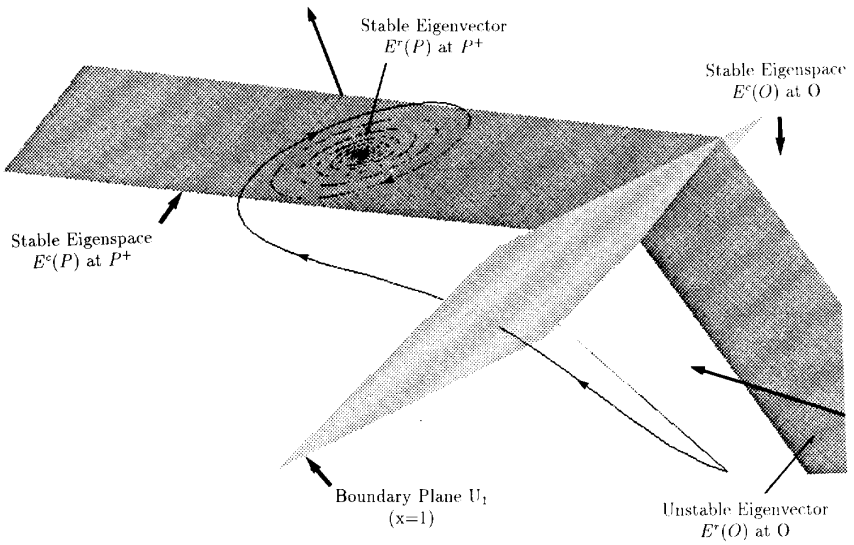

Fig. 5. Stable equilibrium point P^+.

The eigenvalues of $\boldsymbol{M_0}$ are the roots of (11) and are given explicitly by using the following Cardan's formulas:

Let

$$p = e - \frac{d^2}{3}, \qquad q = f - \frac{de}{3} + 2\frac{d^3}{27} \tag{12}$$

where

$$\begin{aligned} d &= k[1 + \gamma + \alpha(1 + a)], \\ e &= \gamma + \beta + \alpha(1 + a)(1 + \gamma) - \alpha, \\ f &= k\alpha[(1 + a)(\gamma + \beta) - \gamma] \end{aligned} \tag{13}$$

Let

$$\begin{aligned} &A = -\frac{q}{2} + \sqrt{\frac{q^2}{4} + \frac{p^3}{27}}, \quad B = -\frac{q}{2} - \sqrt{\frac{q^2}{4} + \frac{p^3}{27}}, \\ &\Delta = 4p^3 + 27q^2. \end{aligned} \tag{14}$$

If $\Delta \geq 0$, we have one real eigenvalue and two complex-conjugate eigenvalues. In this case, roots of (11) are given by

$$\begin{aligned} \lambda_1 &= \sqrt[3]{A} + \sqrt[3]{B} - \frac{d}{3} \\ \lambda_2 &= -\frac{\sqrt[3]{A} + \sqrt[3]{B}}{2} - \frac{d}{3} + j\sqrt{3}\frac{\sqrt[3]{A} - \sqrt[3]{B}}{2} \\ \lambda_3 &= -\frac{\sqrt[3]{A} + \sqrt[3]{B}}{2} - \frac{d}{3} - j\sqrt{3}\frac{\sqrt[3]{A} - \sqrt[3]{B}}{2}. \end{aligned} \tag{15}$$

If $\Delta < 0$, we have three real eigenvalues. In this case, roots of (11) are given by

$$\begin{aligned} \lambda_1 &= 2\sqrt{\frac{-p}{3}}\cos\frac{\Phi}{3} - \frac{d}{3} \\ \lambda_2 &= 2\sqrt{\frac{-p}{3}}\cos\left(\frac{\Phi}{3} + 120^\circ\right) - \frac{d}{3} \\ \lambda_3 &= 2\sqrt{\frac{-p}{3}}\cos\left(\frac{\Phi}{3} + 240^\circ\right) - \frac{d}{3} \end{aligned} \tag{16}$$

where $\cos\Phi = \frac{\sqrt{27}q}{2p\sqrt{-p}}$, and Φ is taken in the first or second quadrant, depending on whether q is negative or positive, respectively.

For the *outer* regions, we simply replace a with b.

2.3. Eigenspaces

Each real eigenvector $\boldsymbol{X}_{\lambda_R}$, corresponding to a real eigenvalue λ_R, is determined up to a multiplicative constant by:

$$\boldsymbol{M_0}\boldsymbol{X}_{\lambda_R} = \lambda_R \boldsymbol{X}_{\lambda_R} \tag{17}$$

and a solution of (17) is:

$$\boldsymbol{X}_{\lambda_R} = \begin{bmatrix} \frac{\alpha}{\alpha(1+a)+\frac{\lambda_R}{k}} \\ 1 \\ -\frac{\beta}{\gamma+\frac{\lambda_R}{k}} \end{bmatrix} \tag{18}$$

The eigenspace, henceforth called the eigenplane corresponding to the complex-conjugate eigenvalues $\lambda_{C\pm} = u \pm jv$, is determined as a linear combination of the two real vectors $\boldsymbol{U}$ and $\boldsymbol{V}$ such that:

$$\begin{pmatrix} \boldsymbol{M_0} - u\boldsymbol{I} & -v\boldsymbol{I} \\ v\boldsymbol{I} & u\boldsymbol{I} - \boldsymbol{M_0} \end{pmatrix} \begin{bmatrix} \boldsymbol{U} \\ \boldsymbol{V} \end{bmatrix} = 0 \tag{19}$$

where $\boldsymbol{X}_{C\pm} = \boldsymbol{U} \pm j\boldsymbol{V}$ is the complex eigenvector corresponding to the complex-conjugate eigenvalues $\lambda_{C\pm}$. This system can be solved either analytically or numerically. For the *outer* region D_1 we simply replace a with b. We can find the eigenvectors and the associated eigenplane of the region D_{-1} by using the odd symmetry of the vectorfield defined by (3).

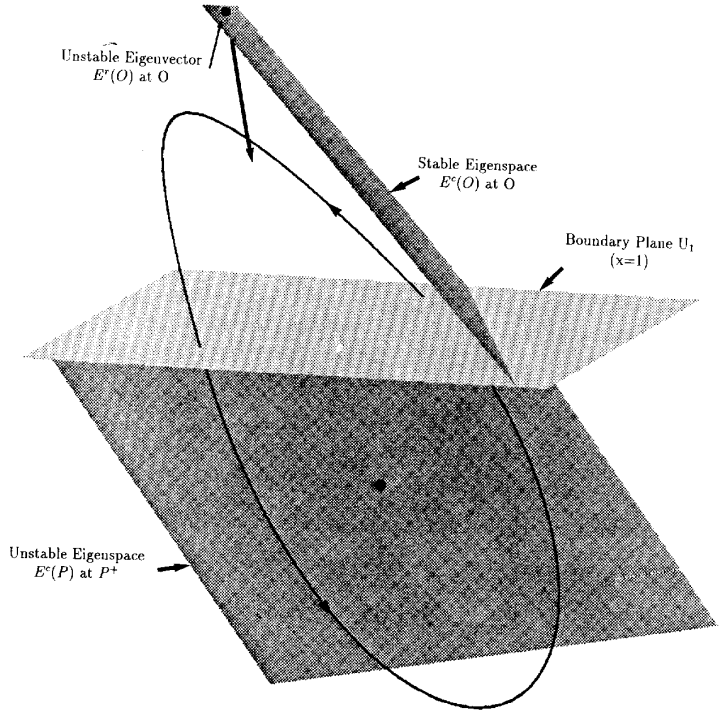

Fig. 6. (a) Period-1 limit cycle ($\alpha = 8.8$).

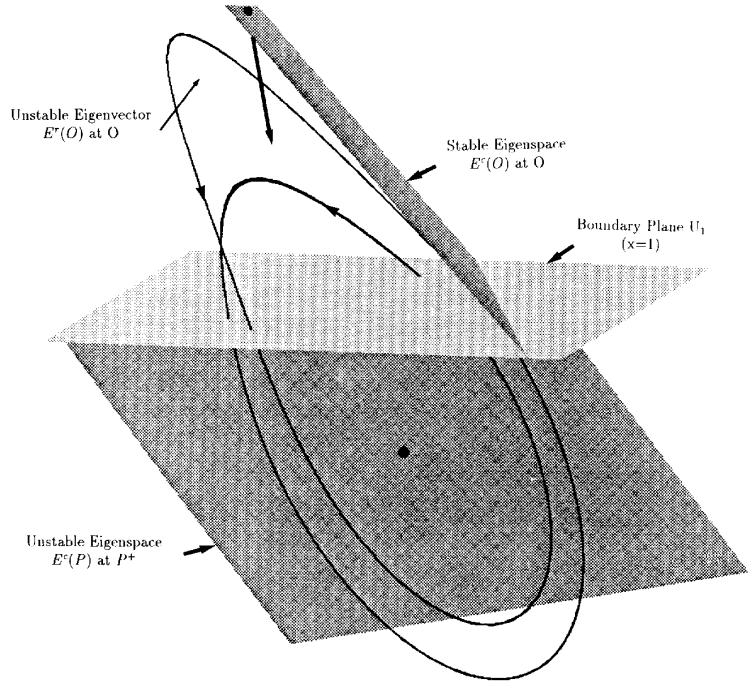

Fig. 6. (b) Period-2 limit cycle ($\alpha = 9.05$).

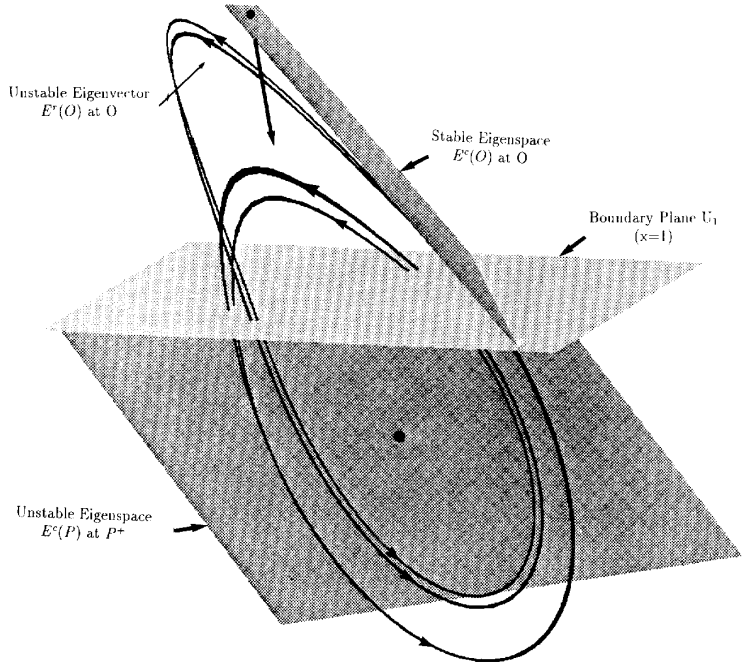

Fig. 7. (a) Period-4 limit cycle ($\alpha = 9.12$).

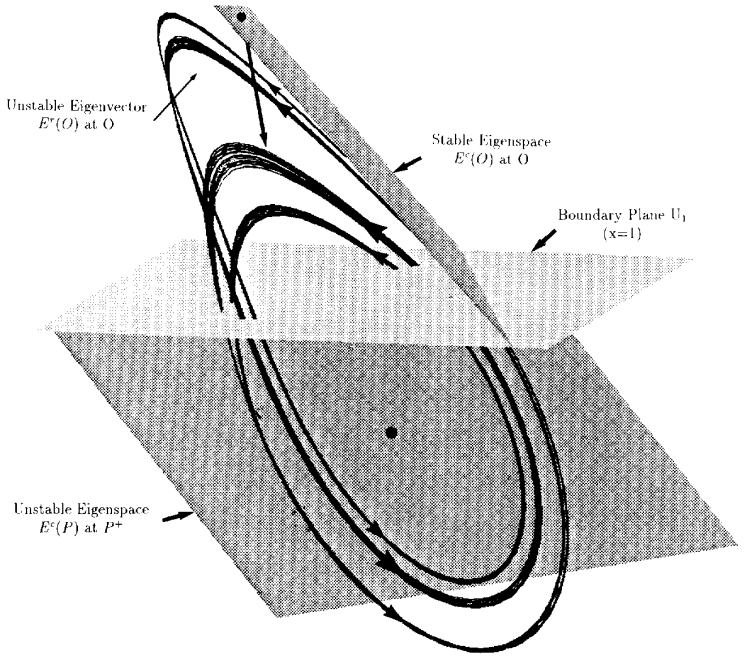

Fig. 7. (b) Period-8 limit cycle ($\alpha = 9.162$). The trajectories squeezed within a narow band around each loop are transients converging toward the limit cycle.

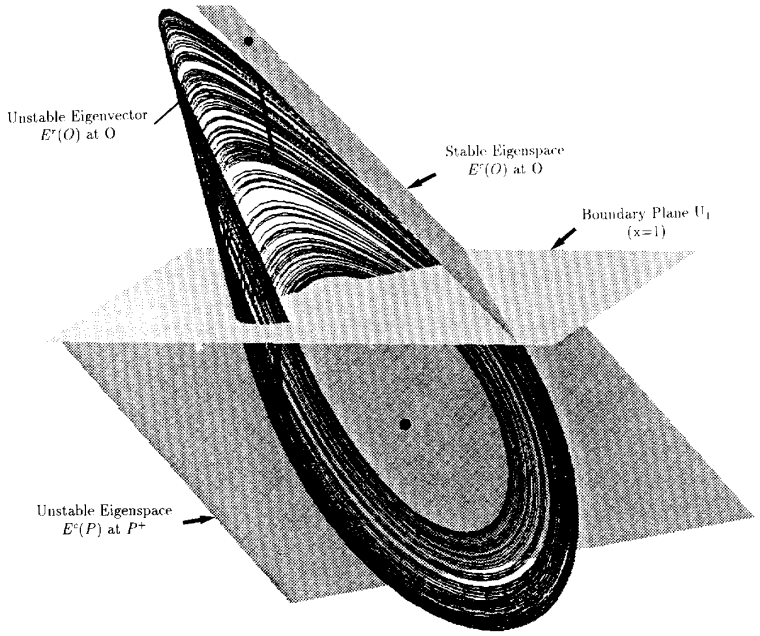

Fig. 8. (a) Spiral Chua's attractor ($\alpha = 9.3$).

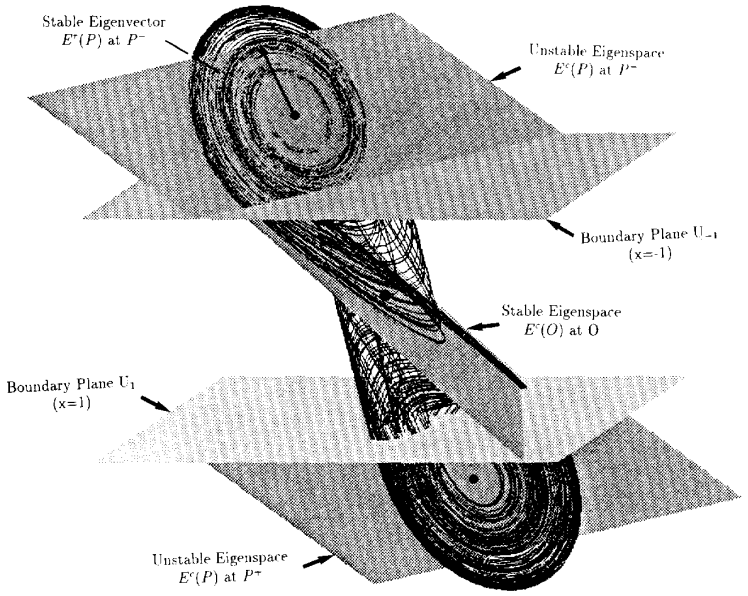

Fig. 8. (b) Double-scroll Chua's attractor ($\alpha = 9.8$).

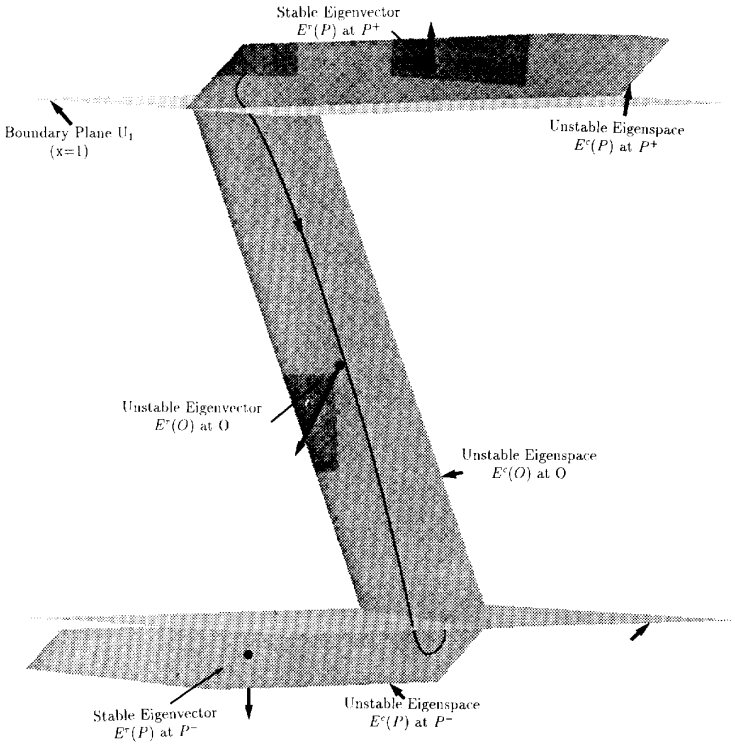

Fig. 9. (a) $\beta = 59.988002$.

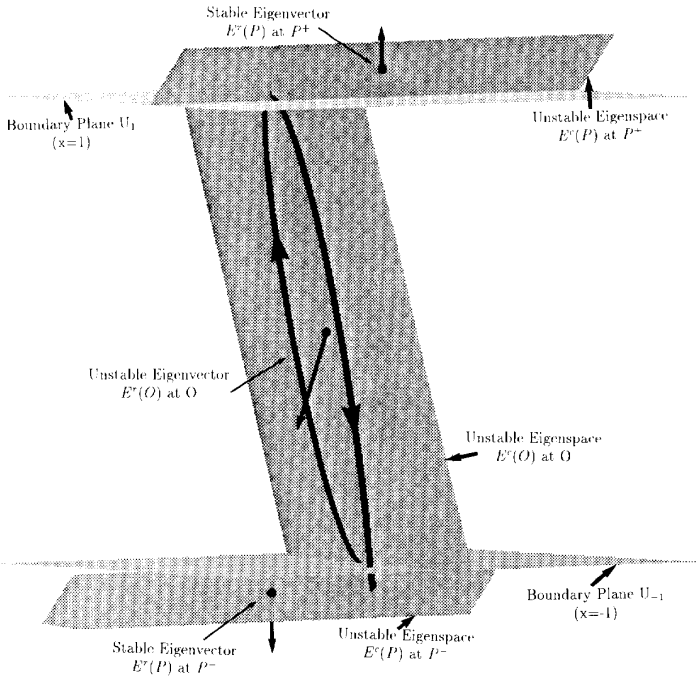

Fig. 9. (b) $\beta = 44.802867$.

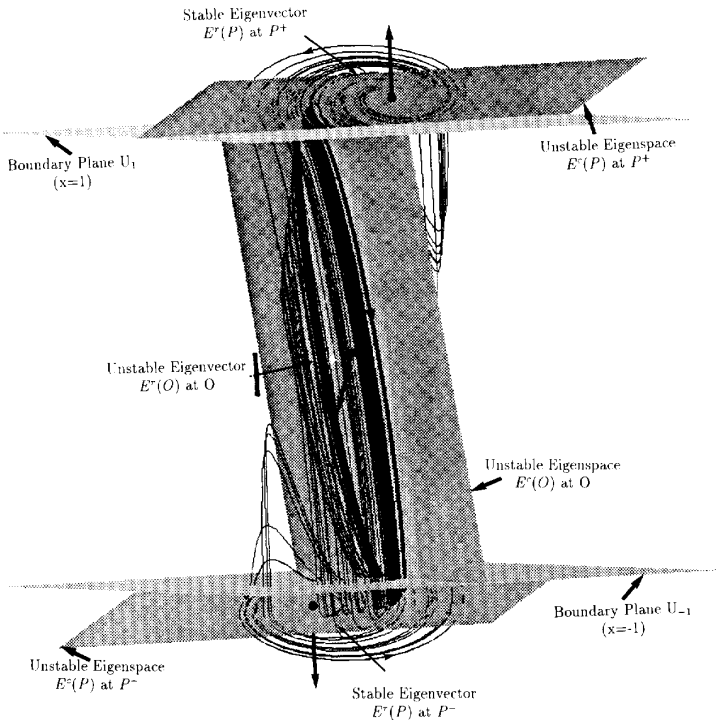

Fig. 10. (a) $\beta = 43.994721$.

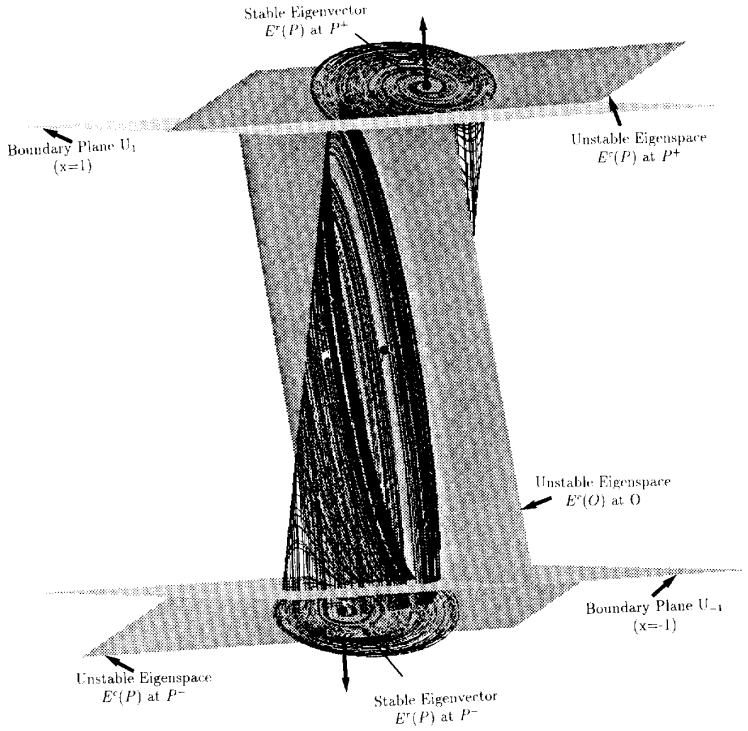

Fig. 10. (b) $\beta = 34.722222$.

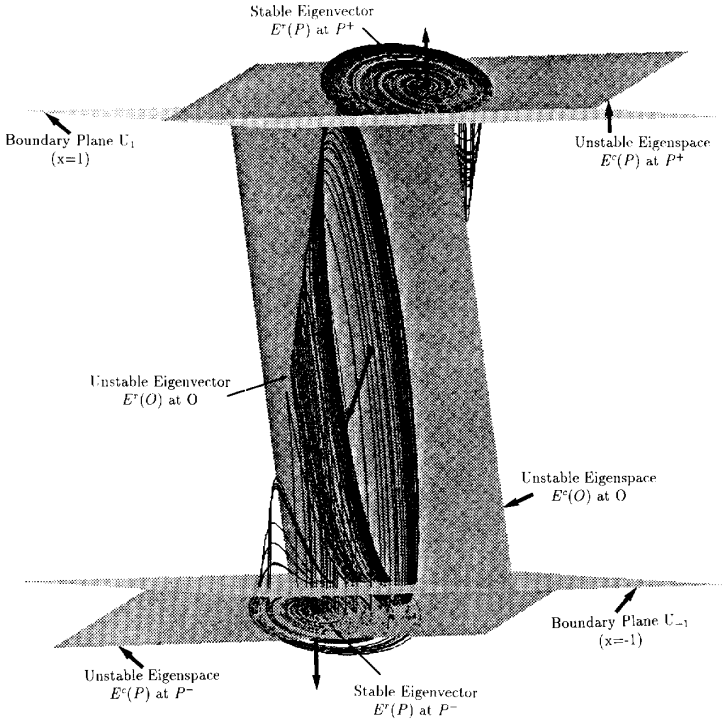

Fig. 11. (a) $\beta = 31.746032$.

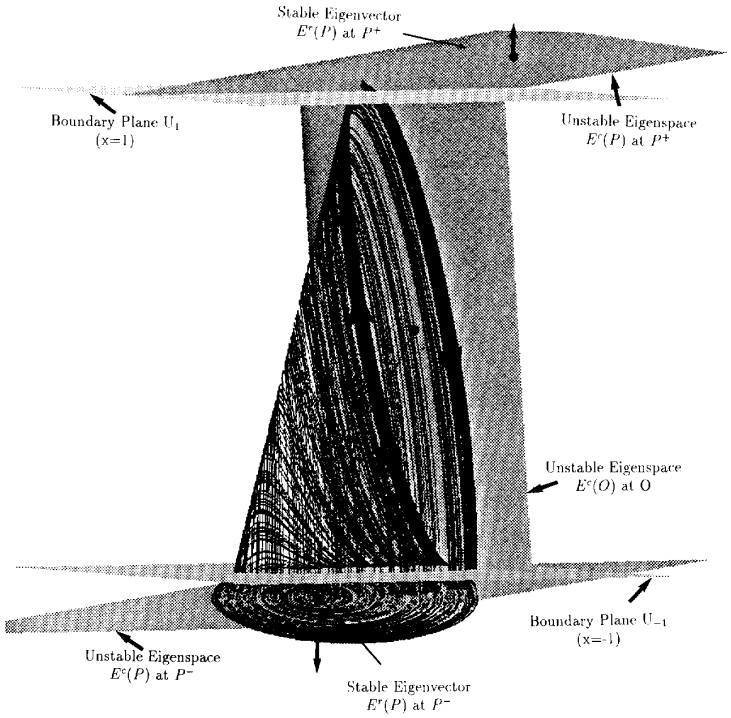

Fig. 11. (b) $\beta = 31.25$.

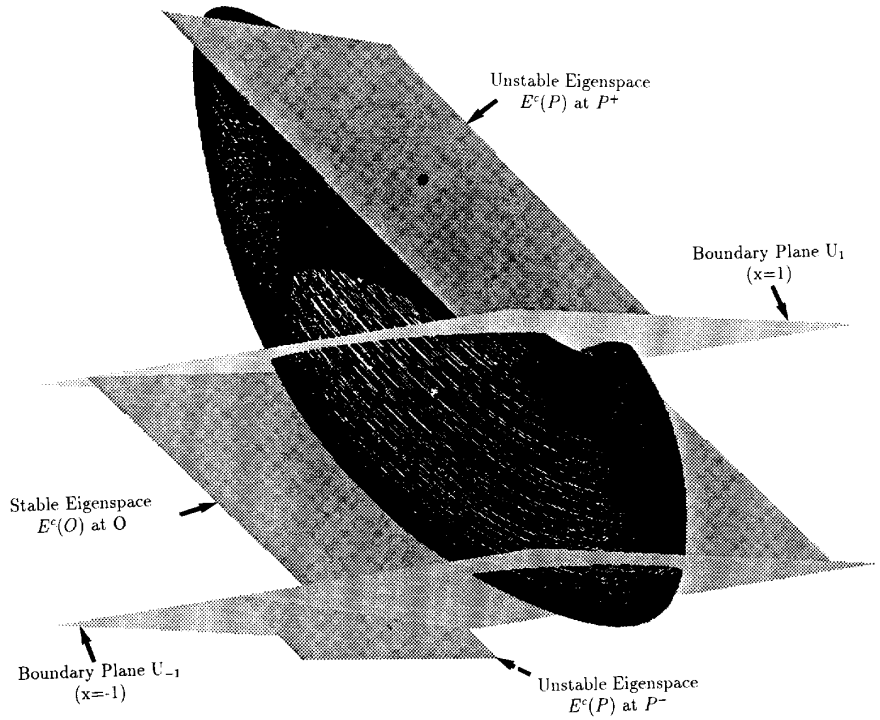

Fig. 12. (a) $\alpha = 100$.

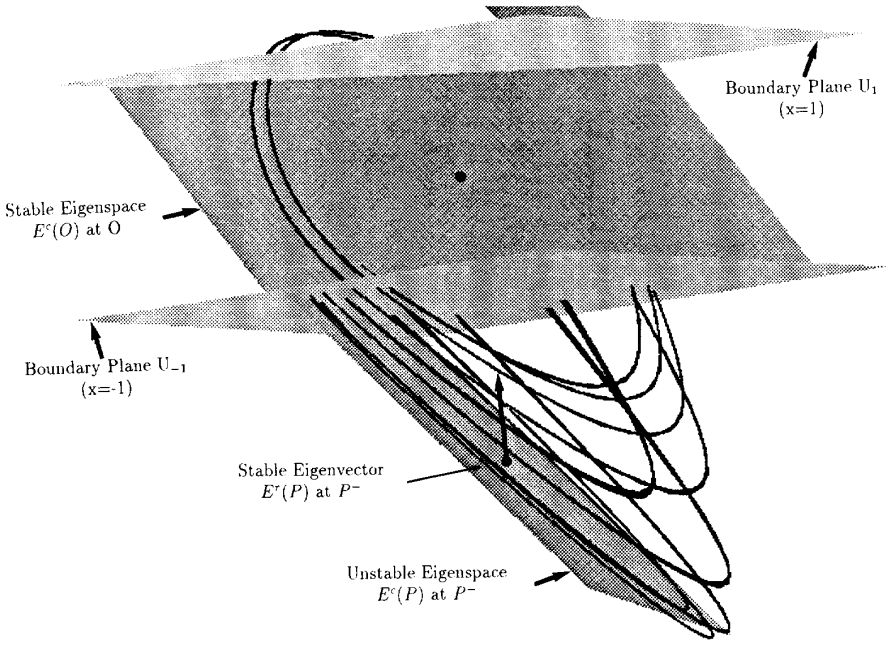

Fig. 12. (b) $\alpha = 166.66667$.

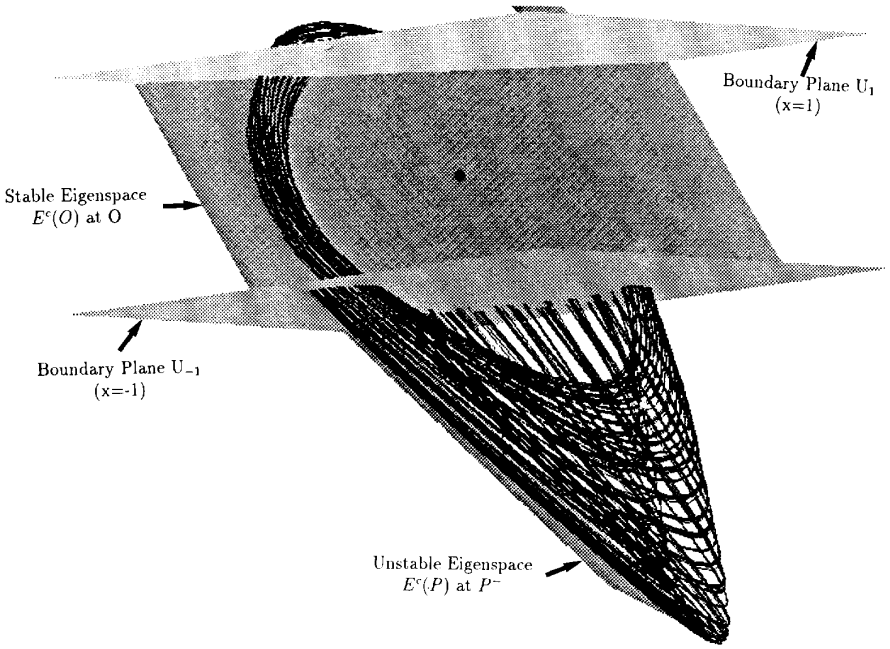

Fig. 13. (a) $\alpha = 196.07843$.

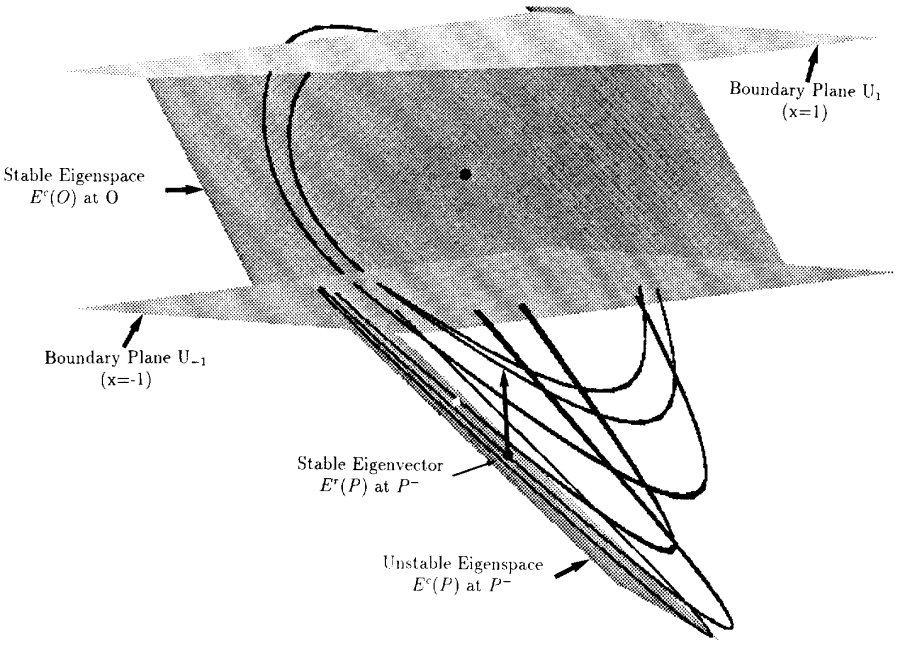

Fig. 13. (b) $\alpha = 200$.

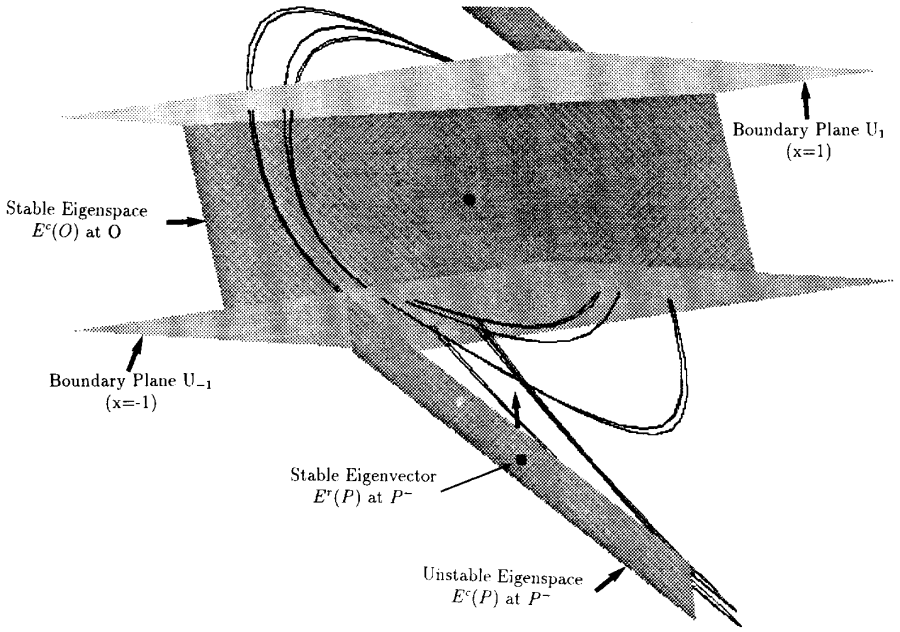

Fig. 14. (a) $\alpha = 285.71429$.

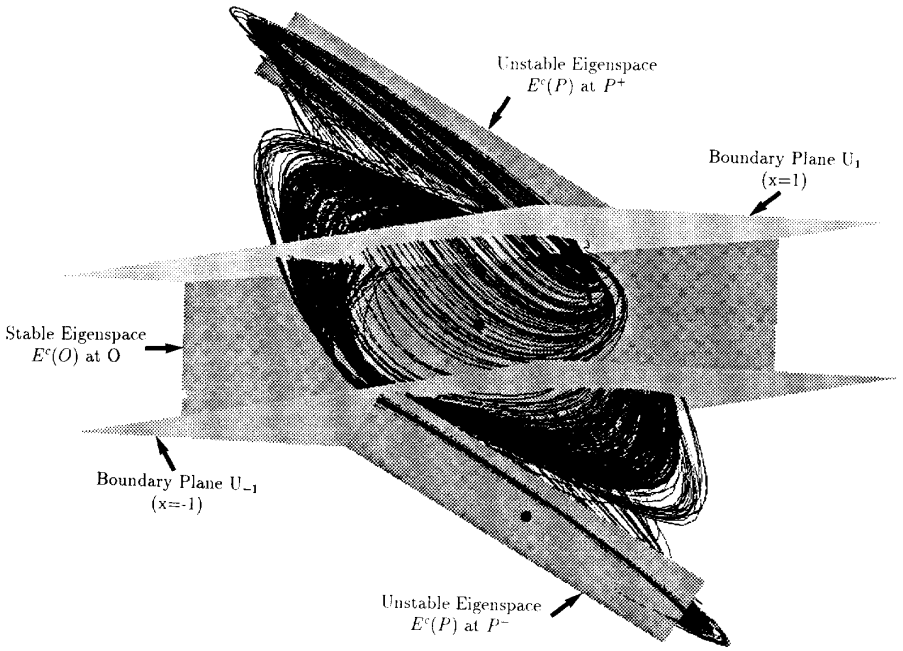

Fig. 14. (b) $\alpha = 340.13605$.

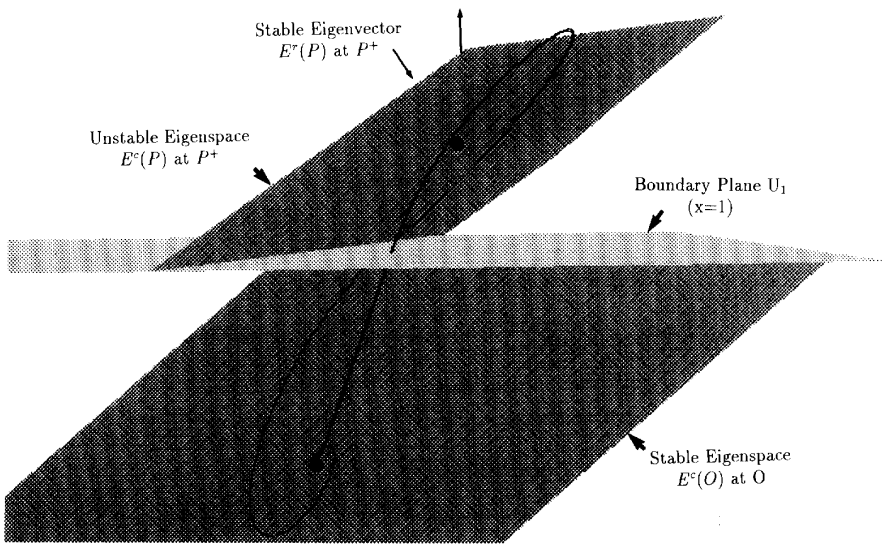

Fig. 15. Homoclinic orbit.

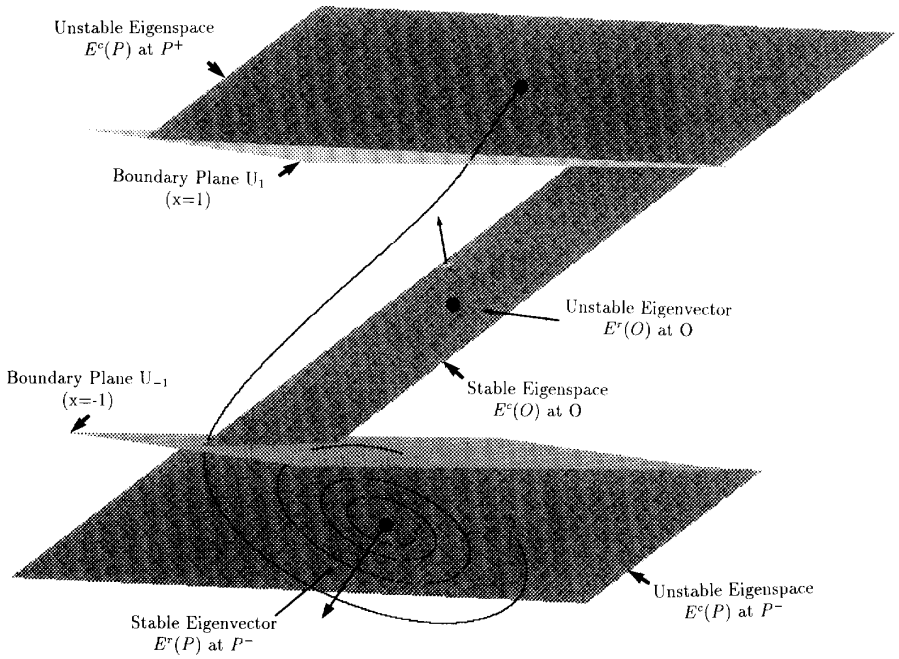

Fig. 16. Heteroclinic orbit.

III. Snapshots

In this section, we present seven sequences of snapshots, each one illustrating an important evolution route to chaos. The snapshots in each sequence are identified by consecutive figure numbers whose associated parameters are collected in Table I.

The following *dimensionless* system

$$\begin{cases} \dot{x} = k\alpha(y - f(x)) \\ \dot{y} = k(x - y + z) \\ \dot{z} = k(-\beta y - \gamma z) \end{cases} \tag{20}$$

where

$$f(x) = bx + \tfrac{1}{2}(a - b)[|x + 1| - |x - 1|] \tag{21}$$

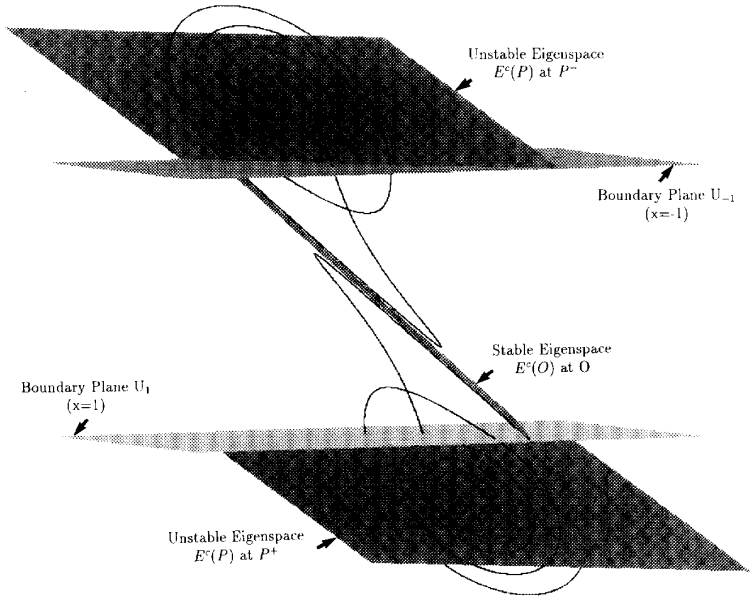

Fig. 17. Just before the collision ($\beta = 13.925$).

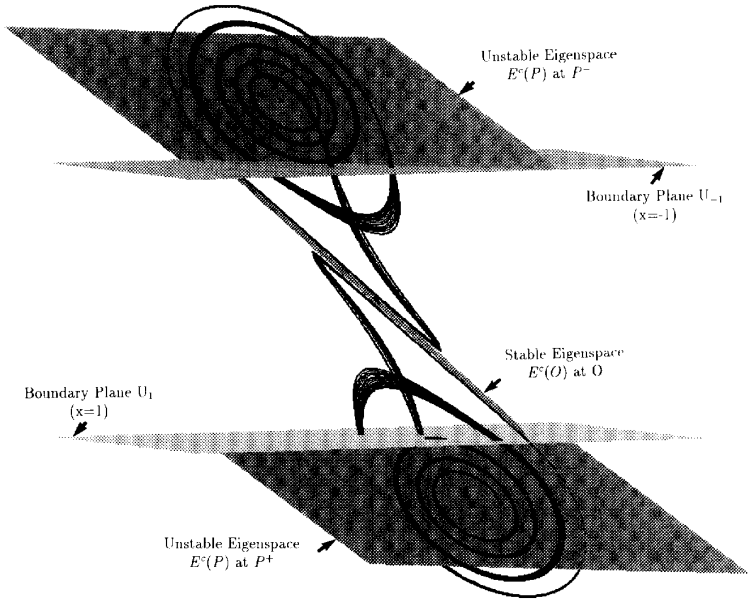

Fig. 18. Just before the collision ($\beta = 13.924$).

has been used to obtain the snapshots shown in Figs. 2–20.

3.1. Snapshots Showing the Time Evolution of the Double-Scroll Chua's Attractor

Figs. 2–4 show the time evolution of the double-scroll Chua's attractor.

3.2. Snapshots of Period-Doubling Route to Chaos

For the parameter values given in the second row (Fig. 5) of Table I, the equilibrium point P^+ is a *stable focus*. Fig. 5 shows a typical trajectory starting from a point in the basin of attraction of P^+ and converging toward P^+.

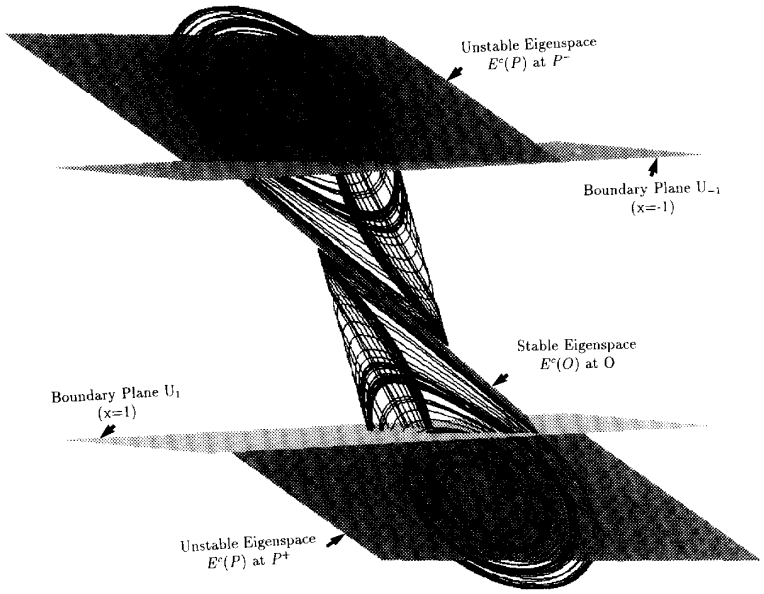

Fig. 19. Just before the collision ($\beta = 13.923$).

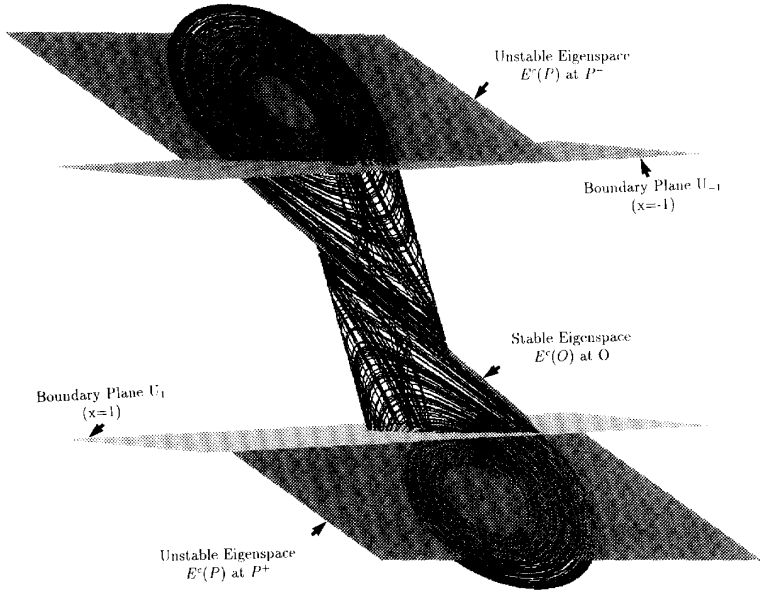

Fig. 20. Just after the collision ($\beta = 13.833$).

By tuning α and/or β, P^+ becomes unstable on crossing the "Hopf bifurcation curve" and gives rise to a limit cycle henceforth referred to as a *period-1 limit cycle*. Figs. 6–8 show the evoluiton of the trajectories from the period-1 limit cycle to the double-scroll Chua's attractor.

3.3. Snapshots of Intermittency Route to Chaos

Figs. 9–11 show the evolution of the trajectories along the intermittency route to chaos. Observe that although the bifurcation scenario shown in Figs. 9–11 involves tuning two parameters (β and α), the intermittency route to chaos is nevertheless a *co-dimension-one* bifurcation in the sense that the corresponding route in the parameter space is a 1-D curve. Indeed, in the original (unnormalized) Chua's oscillator with which Figs. 9–11 are associated [2], only the inductance L is tuned. However, in the corresponding *dimensionless* circuit, both parameters β and α depend on L, and hence, both parameters must be tuned as shown in Table I in order to obtain the corresponding intermittency route depicted in [2].

3.4. Snapshots of Torus Breakdown Roūte to Chaos

Figs. 12–14 show the torus breakdown to chaos.

3.5. Snapshot of a Homoclinic Orbit

Fig. 15 shows a homoclinic orbit.

3.6. Snapshot of a Heteroclinic Orbit

Fig. 16 shows a heteroclinic orbit.

3.7. Snapshots Showing Collision Between Two Spiral Chua's Attractors

Figs 17–20 show a collision between two spiral Chua's attractors.

REFERENCES

[1] L. O. Chua, "The genesis of Chua's circuit," *Archiv für Elektronik und Übertragungstechnik*, vol. 46, pp. 250–257, 1992.
[2] ——, "Global unfolding of Chua's circuit," *IEICE Trans. Fundamentals Electron. Commun. Comput. Sci.*, vol. E76-A, pp. 704–734, 1993.
[3] ——, "A simple ODE with more than 20 strange attractors," *Proc. World Cong. Nonlinear Analysts* (Tampa, FL), Aug. 19–26, 1992.
[4] R. N. Madan (Guest Ed.), *J. Circuits Syst. Comput.: Special issue on Chua's circuit: A paradigm for chaos*, vol. 3, Mar. 1993, pt. I.
[5] ——, *J. Circuits, Syst. Comput.: Special issue on Chua's circuit: A paradigm for chaos*, vol. 3, June 1993, pt. II,.
[6] P. Deregel, "Chua's oscillator: A zoo of attractors," *J. Circuits, Syst. Comput.*, vol. 3, June 1993.
[7] M. P. Kennedy, "Robust op amp realization of Chua's circuit," *Frequenz*, vol. 46, pp. 66–80, 1992.

Philippe Kévorkian received the master's degree in physics (with distinction) from the University of Paris in 1991. He received the engineering diploma from l'Ecole Nationale Supérieure de l'Aéronautique et de l'Espace, France, in 1993. He is currently studying for a Diplôme d'Etudes Approfondies in applied mathematics.